
Uncertainty-aware Evaluation of Auxiliary Anomalies with the Expected Anomaly Posterior

Lorenzo Perini*
DTAI lab & Leuven.AI,
KU Leuven, Belgium

Maja Rudolph
Bosch Center for AI, USA
University of Wisconsin-Madison, USA

Sabrina Schmedding
Bosch Center for AI, Germany

Chen Qiu
Bosch Center for AI, USA

Abstract

Anomaly detection is the task of identifying examples that do not behave as expected. Because anomalies are rare and unexpected events, collecting real anomalous examples is often challenging in several applications. In addition, learning an anomaly detector with limited (or no) anomalies often yields poor prediction performance. One option is to employ auxiliary synthetic anomalies to improve the model training. However, synthetic anomalies may be of poor quality: anomalies that are unrealistic or indistinguishable from normal samples may deteriorate the detector’s performance. Unfortunately, no existing methods quantify the quality of auxiliary anomalies. We fill in this gap and propose the expected anomaly posterior (EAP), an uncertainty-based score function that measures the quality of auxiliary anomalies by quantifying the total uncertainty of an anomaly detector. Experimentally on 40 benchmark datasets of images and tabular data, we show that EAP outperforms 12 adapted data quality estimators in the majority of cases.

1 Introduction

Anomaly detection aims at identifying the examples that do not conform to the normal behaviour [6]. Anomalies are often connected to adverse events, such as defects in production lines [52], excess water usage [38], failures in petroleum extraction [33], or breakdowns in wind turbines [37]. Detecting anomalies in time can reduce monetary costs and protect resources from harm. For this reason, there has been significant effort to develop data-driven methods for anomaly detection.

Unfortunately, anomalies are inherently rare and sparse, which makes collecting them hard. As a result, the data used to train data-driven methods for anomaly detection only contains a limited number of anomalies. In autonomous driving, for instance, sensor malfunctions or unexpected pedestrian movements are infrequent but critical to address. As an additional challenge, available anomalies rarely represent all potential cases due to the unpredictable nature of these events. In financial fraud detection, new techniques and schemes are constantly emerging, meaning previously identified anomalies do not cover future fraudulent methods. These factors highlight the difficulty of obtaining comprehensive anomaly datasets, as new and unpredictable anomaly types are inherent to the very nature of these events.

With recent improvements in generative modeling (e.g. [19, 10]) it seems natural to introduce auxiliary anomalies, e.g. for training an anomaly detector [35], or for model selection [12]. However, there are several failure cases for generated anomalies that should not be neglected. For one, auxiliary

*Work done during the internship at Bosch Center for AI. Correspondence: lorenzo.perini@kuleuven.be

anomalies might be too similar to normal examples. For instance, the defects introduced into images of products might be imperceptible, making the image indistinguishable from a normal counterpart. On the other hand, the quality of a generated anomaly also deteriorates as it becomes too unrealistic, e.g. when the generated defect of a product is too severe. Including poor-quality anomalies for training a model is likely to harm its performance [18, 42, 29, 30]. Although Chen et al. [8], Ming et al. [34] proposed sampling methods for selecting informative anomalies during training, there is no approach for quantifying the quality of auxiliary anomalies.

In this paper, we close this critical gap by introducing the **Expected Anomaly Posterior (EAP)**, the first example-wise score function that measures the quality of auxiliary anomalies. Our approach relies on a fundamental insight: high-quality auxiliary anomalies must fulfill two criteria — they must be (1) distinguishable from normal examples in the training data and (2) realistic, i.e. similar to the training examples (e.g., scratches only affect few pixels, leaving an anomalous image relatively similar to a normal one). Finding a balance between these two characteristics poses an inherent challenge. On one hand, auxiliary anomalies risk deteriorating an anomaly detector’s performance if they closely resemble normal examples. On the other hand, they become less useful the more dissimilar from the training data.

Building upon this insight, we adopt a Bayesian framework to model the uncertainty of a detector’s prediction. This framework accounts for both an example’s dissimilarity from the normal class (via class-conditional probability) and its realism (via example density). The expectation of the posterior probability that an example is anomalous reflects our concept of the quality of an auxiliary anomaly: the approximation we derive in Section 3 to compute the EAP will give lower scores to indistinguishable and unrealistic anomalies.

In summary, we make three following contributions.

- In Section 3, we compute the expected anomaly posterior (EAP), which measures the quality of an anomaly by accounting both for aleatoric and epistemic uncertainty.
- In Section 4, we provide a theoretical analysis of EAP, including its properties and guarantees.
- In Section 5, we run an extensive experimental analysis and show that EAP enhances a detector’s performance when using high-quality anomalies to enrich training or perform model selection.

2 Related Work

Anomaly detection. Designing an anomaly detector requires developing a way to assign real-valued anomaly scores to the examples [6, 17], where the higher the score, the more anomalous the example. Existing approaches often rely on heuristic intuitions about expected anomalous behavior [36, 39]. Propagation-based detectors, such as those using proximity to training examples, assume similar instances share the same label (e.g., SSDO) [47]. Loss-based detectors, on the other hand, learn a decision boundary (e.g., a hypersphere over normals) and assign scores based on the distance to this boundary [43, 55, 13, 41]. Self-supervised detectors learn models through solving auxiliary tasks and score anomalies according to model performance on self-supervised tasks [15, 4, 40]. Recently, foundation models have enabled zero-shot anomaly detection [21], which overcomes the need to collect anomalies for training but still requires their use in model selection [12].

Data quality. Traditional quality score functions evaluate training examples by (1) defining a utility function that takes as input a subset of the training set and measures the performance of the model, and (2) finding a function that assigns a score to an example by quantifying its impact on the model’s performance when included/excluded for training [53, 23]. Methods like leave-one-out (LOO) iteratively remove one example at a time to observe how test performance varies. Various techniques, such as DATASHAP [14], BETASHAP [27], KNNSHAP [22], DATA BANZHAF [50], and AME [31], compute the marginal contribution of an example by bootstrapping the training set and assessing its impact on model training. DATA OOB is an out-of-bag (OOB) evaluator that measures out-of-bag accuracy variation. Other methods like LAVA and influence functions (INF) quantify how the utility changes when a specific example is more weighted. The Supplement A.1 provides a detailed overview. Unfortunately, all existing data quality estimators focus on evaluating the impact of training examples and are not tailored to estimate the quality of an external anomaly.

3 Methodology

In this Section, we introduce the problem setup and notations (Section 3.1), and describe our proposed approach for quantifying the quality of auxiliary anomalies (Section 3.2).

3.1 Problem setup

Let $(\Omega, \mathcal{F}, \mathbb{P})$ be a probability space, and $X: \Omega \rightarrow \mathbb{R}^d, Y: \Omega \rightarrow \{0, 1\}$ two random variables representing, respectively, feature vectors and class labels (0 for normals, 1 for anomalies). A training dataset is an i.i.d. sample of pairs $D = \{(x_1, y_1), \dots, (x_n, y_n)\} \sim \mathbb{P}(X, Y)$ drawn from the joint distribution. Because of the rarity of anomalies, we assume to have only $m \ll n$ (labeled) examples from the anomaly class, in addition to $n - m$ (labeled) normal examples.

Since anomalies provide valuable training signals, but are so rare to acquire, Hendrycks et al. [18], Murase and Fukumizu [35] propose using auxiliary anomalies during training. With significant improvements in generative modeling, there are many candidate methods for generating synthetic anomalies to complement the training data. Our goal is to evaluate candidate synthetic anomalies with a quality score function ϕ such that higher scores indicate that the synthetic anomaly is useful for training a detector. Before formalizing our research task, we introduce the following definition.

Definition 3.1 (Categorization of Anomalies). Given the examples $x_R, x_U, x_I \in \mathbb{R}^d$, we define that

- x_R is a *realistic anomaly* if it has high conditional probability and non-zero density

$$\mathbb{P}(Y = 1|X = x_R) \in [0.5, 1] \text{ and } \mathbb{P}(X = x_R) > 0;$$

- x_U is an *unrealistic anomaly* if it has high conditional probability and null density

$$\mathbb{P}(Y = 1|X = x_U) \in [0.5, 1] \text{ and } \mathbb{P}(X = x_U) = 0;$$

- x_I is an *indistinguishable anomaly* if it has null conditional probability and non-zero density

$$\mathbb{P}(Y = 1|X = x_I) = 0 \text{ and } \mathbb{P}(X = x_I) > 0.$$

An anomaly detector is a function $f: \mathbb{R}^d \times \{0, 1\} \rightarrow \mathbb{R}$ that assigns a real-valued anomaly score $f(x)$ to any $x \in \mathbb{R}^d$. The detector f is learned using the training set D , and can be used for estimating the conditional probability $\mathbb{P}(Y|X)$ by mapping the scores to $[0, 1]$ [26].

Given: D with $m \ll n$ anomalies, a set of l auxiliary anomalies $\{x \in \mathbb{R}^d\}$, and a detector f ;

Challenge: Design a quality score function $\phi: \mathbb{R}^d \rightarrow \mathbb{R}$ for the auxiliary anomalies, such that for any realistic anomaly $x_R \in l$ and any unrealistic or indistinguishable anomaly $x_U, x_I \in l$, the realistic anomaly has a higher quality score $\phi(x_R) > \phi(x_U), \phi(x_I)$.

With this categorization, estimators for $\mathbb{P}(Y|X)$ alone cannot differentiate between x_R and x_U , while estimators for $\mathbb{P}(X)$ alone cannot differentiate between x_R and x_I , thus not qualifying as good quality estimators. Intuitively, a score must quantify the conditional probability to distinguish between x_R and x_I but the estimate needs to account for an example’s density. Roughly speaking, the lower an example’s density the more uncertain the estimate, because the lack of similar training data prevents a model from learning the correct probability. This introduces an additional level of uncertainty (namely, epistemic), which requires a Bayesian perspective to be properly measured [20, 2].

3.2 The Expected Anomaly Posterior

Capturing a detector’s uncertainty is challenging because one needs to account for (1) the example’s proximity to the normal class (i.e., the aleatoric uncertainty) and (2) the lack of training data in the region where the example falls (i.e., the epistemic uncertainty). This is particularly complicated in anomaly detection because the epistemic uncertainty tends to be high for most anomalies, as they often fall in low-density regions [3].

We propose EAP, a novel approach that estimates the quality of auxiliary anomalies by capturing an anomaly detector’s uncertainty. The key idea is to model each example’s probability of being an anomaly p_x . The quality score we propose is the expected posterior of this parameter.

Assumption. For any x the class conditional distribution $Y = 1|X = x$ is a Bernoulli

$$\mathbb{P}(Y|X = x) = \text{BERNOULLI}(p_x), \quad p_x \sim \text{BETA}(\alpha_0, \beta_0).$$

The parameter p_x can be interpreted as the probability of the example x being an anomaly. With the Beta prior we can incorporate prior knowledge such as the expected ratio of anomalies in the data [38]. Since we have at most one observation of Y for each x , we follow Charpentier et al. [7] and model the posterior over p_x by conditioning on pseudo observations. Given N pseudo observations $\bar{y}_1, \dots, \bar{y}_N$ hypothetically drawn from $\mathbb{P}(Y|X = x)$, the posterior,

$$p_x|\bar{y}_1, \dots, \bar{y}_N \sim \text{BETA}(\alpha_0 + \alpha_1, \beta_0 + N - \alpha_1), \quad (1)$$

is conjugate to the Beta prior, where $\alpha_1 = \sum_{i=1}^N \mathbb{1}(\bar{y}_i = 1)$ is the number of anomalies in the pseudo observations. That is, if we could sample N labels for the same example x , i.e. $(x, y_1), \dots, (x, y_N)$, we would derive the posterior distribution of $Y|X = x$ by using a simple Bayes update (Eq. 1). However, sampling N labels for the same example x is practically impossible. Thus, we need to parametrize α_1 . Roughly speaking, if we drew n training examples from $\mathbb{P}(X, Y)$ we would expect to draw $N = n \cdot \mathbb{P}(X = x)$ examples with features x , among which $\mathbb{P}(Y = 1|X = x)$ are anomalies:

$$\alpha_1 \approx n \times \widehat{\mathbb{P}(Y = 1, X = x)} \approx n \times \underbrace{\widehat{\mathbb{P}(Y = 1|X = x)}}_{\text{conditional probability}} \times \underbrace{\widehat{\mathbb{P}(X = x)}}_{\text{data density}} \quad (2)$$

where $\hat{\cdot}$ indicates that the quantity is estimated. We describe how we compute both terms below. The expectation of the posterior in Equation (1) reflects the quality of an auxiliary anomaly x : if the expected posterior is high, the evidence is enough to rely on the expected conditional probability for evaluating the auxiliary anomaly, while if it is low, the quality reflects our prior belief.

Estimating the data density. Computing $\widehat{\mathbb{P}(X = x)}$ has two main challenges. First, most traditional density estimators suffer the well-known curse of dimensionality [48, 1]. Second, deep estimators (e.g., Normalizing Flows [25]) are prohibitively time-consuming to be employed for data quality scores. Thus, EAP relies on the rarity score [16], which is fast to compute and weakly affected by the curse of dimensionality. The rarity score (1) creates k -NN spheres centered on each training example, and (2) assigns the smallest radius of the sphere that contains the given synthetic example. If the synthetic example falls outside of all spheres, it is considered too uncommon and gets null rarity.

We use the rarity score $r_{\hat{k}}$ with an estimated \hat{k} to estimate the data density.² Intuitively, the density behaves as the inverse of the rarity score: highly uncommon examples should have low density. Thus, we take the reciprocal value of the rarity score and normalize it using the training rarity scores:

$$\widehat{\mathbb{P}(X = x)} = \frac{1/r_{\hat{k}}(x)}{1/r_{\hat{k}}(x) + \sum_{i=1}^n 1/r_{\hat{k}}(x_i)}. \quad (3)$$

Estimating the conditional probability. Computing $\widehat{\mathbb{P}(Y = 1|X = x)}$ in anomaly detection is a hard task because (1) class probabilities are generally unreliable for imbalanced classification tasks [49, 46], and (2) the available anomalies might be non-representative of the whole anomaly class (i.e., we have access to a biased set). This makes traditional calibration techniques often impractical [44, 9]. However, we mainly care about having probabilities that satisfy two properties. First, they must be coherent with the detector’s prediction, namely a predicted anomaly (normal) needs a probability greater (lower) than 0.5. Second, we want the proportion of predicted anomalies to match the expected proportion of true anomalies. This guarantees that, if the detector’s ranking is accurate, the class predictions are optimally computed.

For this task, we employ a squashing scaler [47] to map the anomaly scores to $[0, 1]$ probability values

$$\widehat{\mathbb{P}(Y = 1|X = x)} = 1 - 2^{-\left(\frac{f(x)}{\lambda}\right)^2} \quad (4)$$

where λ is the detector’s decision threshold which we set such that the number of training examples with probability > 0.5 (after mapping) is equal to the number of training anomalies m [38].

²We explain how we compute \hat{k} in Appendix A.2 in the Supplement.

Computing the quality scores. Using our point estimates for the data density and the conditional probability, the parametrized posterior distribution $p_x|\bar{y}_1, \dots, \bar{y}_N$ can be computed by substituting $\alpha_1 = n\overline{\mathbb{P}(Y=1|X=x)\mathbb{P}(X=x)}$ and $N = n\overline{\mathbb{P}(X=x)}$ to Eq. 1. Finally, we compute the quality of an auxiliary anomaly x by taking its expectation

$$\phi(x) = \mathbb{E}[p_x|\bar{y}_1, \dots, \bar{y}_N] = \frac{\alpha_0 + n\overline{\mathbb{P}(X=x)\mathbb{P}(Y=1|X=x)}}{\alpha_0 + \beta_0 + n\overline{\mathbb{P}(X=x)}}.$$

4 Theoretical Analysis of EAP

We theoretically investigate two tasks. First, we illustrate the main properties of EAP, namely how it behaves when subject to (1) large training sets ($n \rightarrow +\infty$), (2) small training sets or zero-density examples, (3) high-class conditional probabilities. Second, we answer the following question: *Given a realistic anomaly x_R , an indistinguishable anomaly x_I and an unrealistic anomaly x_U as in Definition 3.1, does EAP rank $\phi(x_R) > \phi(x_I), \phi(x_U)$?*

i) EAP has three relevant properties:

P1) Convergence to class conditional probabilities. The number of training examples indicates how strong the empirical evidence is. That is, the detector f has enough evidence to estimate properly the class conditional probability. Thus, for high n , EAP converges to the class conditional probability

$$\phi(x) \rightarrow \overline{\mathbb{P}(Y=1|X=x)} \quad \text{for } n \rightarrow +\infty;$$

P2) Convergence to the prior's mean. No empirical evidence implies that the posterior remains equal to the prior. Thus, EAP assigns the prior's mean for relatively small n or a null-density region,

$$\phi(x) \rightarrow \frac{\alpha_0}{\alpha_0 + \beta_0} \quad \text{for } n \rightarrow 0 \text{ or } \overline{\mathbb{P}(X=x)} \rightarrow 0.$$

P3) The quality of distinguishable anomalies increases with their density. Given $\overline{\mathbb{P}(Y=1|X=x)} \approx 1$ for an example x , its quality depends only on its density: the closer/more similar to the training examples, the higher the density, the higher its quality:

$$\phi(x) \approx 1 - \frac{\beta_0}{\alpha_0 + \beta_0 + n\overline{\mathbb{P}(X=x)}}.$$

ii) EAP' ranking guarantee.

We show that EAP ranks the anomalies as (1st) realistic, (2nd) unrealistic, and (3rd) indistinguishable.

Theorem 4.1. *Let $x_R, x_U, x_I \in \mathbb{R}^d$ be, respectively, a realistic, unrealistic, and indistinguishable anomaly. If the estimators in Eq. 3 and Eq. 4 satisfy the properties of Definition 3.1, then*

$$\frac{\alpha_0}{\alpha_0 + \beta_0} < 0.5 \implies \phi(x_R) > \phi(x_U) > \phi(x_I). \quad (5)$$

Proof. Using the definition of indistinguishable and unrealistic anomaly, we immediately conclude

$$\phi(x_U) = \frac{\alpha_0}{\alpha_0 + \beta_0} > \frac{\alpha_0}{\alpha_0 + \beta_0 + n\overline{\mathbb{P}(X=x_I)}} = \phi(x_I)$$

because $\mathbb{P}(X=x_I) > 0$. As a second step, we assume that $\frac{\alpha_0}{\alpha_0 + \beta_0} < 0.5$ and show algebraically that

$$\begin{aligned} \phi(x_R) > \phi(x_U) &\iff \phi(x_R) - \phi(x_U) > 0 \iff \frac{\alpha_0 + n\overline{\mathbb{P}(X=x_R)\mathbb{P}(Y=1|X=x_R)}}{\alpha_0 + \beta_0 + n\overline{\mathbb{P}(X=x_R)}} - \frac{\alpha_0}{\alpha_0 + \beta_0} > 0 \\ &\iff n\overline{\mathbb{P}(X=x_R)} [(\alpha_0 + \beta_0)\overline{\mathbb{P}(Y=1|X=x_R)} - \alpha_0] > 0 \iff \overline{\mathbb{P}(Y=1|X=x_R)} > \frac{\alpha_0}{\alpha_0 + \beta_0}, \end{aligned}$$

which holds as $\overline{\mathbb{P}(Y=1|X=x_R)} > 0.5 > \frac{\alpha_0}{\alpha_0 + \beta_0}$. \square

5 Experiments

We empirically evaluate three aspects of our method EAP: (a) whether it measures properly the quality of auxiliary anomalies, and (b) its impact on selecting auxiliary anomalies for learning a model or (c) for model selection. To this end, we address the following five experimental questions:

- Q1. How does EAP compare to existing methods at assigning quality scores?
- Q2. How does a model’s performance vary when including *high-quality* anomalies for training?
- Q3. How does a model’s performance vary when including *low-quality* anomalies for training?
- Q4. How does the performance of a CLIP-based zero-shot anomaly detection method vary when using the selected auxiliary anomalies for prompt tuning?
- Q5. How do EAP’ scores vary for different priors?

5.1 Experimental Setup

Baselines. We compare EAP³ with 12 adapted baselines: LOO, KNNSHAP [22], DATA-BANZHAF [50], AME [31], LAVAEV [24], INF [11], and DATAOOB [28] are existing data quality evaluators that measure the impact of a training example on the model performance. We adapt these methods by including each auxiliary anomaly (individually) in the training set and evaluating its contribution. RANDEEV assigns uniform random scores to each auxiliary anomaly. RARITY [16] computes the rarity score of each auxiliary anomaly. Finally, we include the estimators for the data density P_x , the class conditional probability $P_{y|x}$, and a linear combination of them $P_{y|x} + NP_x$.

Data. We carry out our study on 40 datasets, including 15 widely used benchmark image datasets (MVTEC) [5], 3 industrial image datasets for Surface Defect Inspection (SDI) [51], and an additional 22 benchmark tabular datasets for anomaly detection with semantically useful anomalies, commonly referenced in the literature [17]. These datasets vary in size, feature count, and anomaly proportion.

For each dataset, we construct an auxiliary set of l anomalies by combining realistic, indistinguishable, and unrealistic anomalies ($\frac{l}{3}$ each). Realistic anomalies are labeled anomalies provided with the dataset, indistinguishable anomalies are labeled normal examples with swapped labels, and unrealistic anomalies come from other datasets. Specifically, to collect unrealistic anomalies we randomly select 5 datasets out of the 40, subsample them to a specific example count, and fix their dimensionality to d using random projections (either extending or reducing it). *Pseudo-quality* labels “good” and “poor” are assigned to real anomalies and the other two groups, respectively, reflecting the ground truth where real anomalies should have high-quality scores.

Setup. For each dataset, we proceed as follows: (i) We create a balanced test set by adding random normal examples and 50% of available anomalies; (ii) We generate a set of l auxiliary anomalies as described above with $\frac{l}{3} = 40\%$ of available anomalies; (iii) We create a training set by adding 10% of available anomalies and all remaining normal examples to the training set. (iv) We apply all methods to evaluate the external set of anomalies, using the training set for validation when required (as $m \ll n$, we avoid partitioning the training set); To mitigate noise, steps (i)-(iv) are repeated 10 times with different seeds, resulting in a total of 4000 experiments (datasets, methods, seeds). While computing EAP is fast, the baselines have high computational costs because they train a model several times. To run all experiments, we use an internal cluster of six 24- or 32-thread machines (128 GB of memory). The experiments finish in ~ 72 hours.

Models and Hyperparameters. For all baselines, we use SSDO [47] as the underlying anomaly detector f with $k = 10$ and Isolation Forest [32] as prior. When exposed to selected auxiliary anomalies, we employ an SVM with RBF kernel (for images) and a RANDOM FOREST (for tabular data) to make the normal vs. abnormal classification. For images, we use the pre-trained ViT-B-16-SIGLIP [54] to extract the features from images and use them as inputs to EAP and all baselines. Our method EAP has one hyperparameter, namely the prior α_0, β_0 , which we set to $\frac{m}{n}$ (the proportion of anomalies in the training set) and $1 - \frac{m}{n}$. Intuitively, this corresponds to the expected proportion of (real) anomalies if an external dataset was sampled from $\mathbb{P}(X, Y)$. The baselines⁴ have the following

³Code is available at: URL provided upon acceptance.

⁴Code: <https://github.com/opendataval>

hyperparameters: KNNSHAP and RARITY have $k = 10$, DATABANZHAF, AME, INF and DATAOOB use 50 models. All other hyperparameters are set as default [45].

Evaluation Metrics. We employ **four** evaluation metrics. First, we use the Area Under the Receiving Operator Curve (AUC_{QLT}) to evaluate the methods’ ability to rank good-quality examples higher than poor-quality ones based on quality scores compared to the pseudo-quality labels. Second, we qualitatively analyze the impact of using auxiliary anomalies in training a model, showing the learning curves (LC_G) with the number of added anomalies following the ranking of quality scores on the x-axis and the test accuracy on the y-axis. We compute the area under the learning curve up to $\frac{1}{3}$ of ranked anomalies ($AULC_G$) and the test accuracy after including top $\frac{1}{3}$ of ranked anomalies (ACC_G). Similarly, we compute the LC_P following the methods’ inverse ordering and measure the $AULC_P$ of including up to $\frac{2}{3}$ of inversely-ranked anomalies, where lower values are desirable. Also, rankings from 1 (best) to 13 (worst) are assigned for each method in every experiment, which are denoted by a r in front in Table 1.

Table 1: Summary of the results obtained by the 13 methods over 18 image (above) and 22 tabular (below) datasets. Columns 6 – 10 show the ranking values for the 4 metrics employed (columns 2 – 5) and their average. For metrics desiring lower values, we mark with a \downarrow . Overall, EAP achieves the best performance and ranking position for most evaluation metrics as well as the best avg. ranking.

18 IMAGE DATASETS										
EVALUATOR	AUC_{QLT}	$AULC_G$	ACC_G	$AULC_P(\downarrow)$	$rAUC_{QLT}$	$rAULC_G$	$rACC_G$	$rAULC_P$	AVG. RANK	
EAP	0.803	0.717	0.833	0.688	1.99	3.94	3.12	3.66	3.18	
RARITY	0.681	0.698	0.786	0.738	4.21	5.07	5.34	7.96	5.65	
LAVA	0.742	0.665	0.755	0.709	2.70	8.17	7.44	4.71	5.75	
$P_{y x} + NP_x$	0.669	0.700	0.795	0.729	4.80	5.60	5.61	7.13	5.79	
LOO	0.537	0.693	0.777	0.694	7.22	5.86	6.56	6.14	6.44	
RANDOMEV	0.491	0.696	0.793	0.756	8.92	6.21	5.93	9.90	7.38	
DATAOOB	0.505	0.685	0.739	0.668	8.66	7.53	9.55	4.35	7.52	
KNNSHAP	0.509	0.695	0.794	0.754	8.58	6.36	5.95	9.44	7.58	
AME	0.512	0.693	0.793	0.756	8.56	6.42	5.85	9.94	7.69	
INF	0.488	0.681	0.778	0.744	8.87	7.01	6.73	8.55	7.79	
$P_{y x}$	0.494	0.671	0.710	0.644	9.30	8.55	10.62	3.04	7.88	
DATABANZHAF	0.500	0.668	0.775	0.748	8.71	8.01	6.68	8.54	7.98	
P_x	0.502	0.535	0.600	0.733	8.59	12.37	11.72	7.72	10.10	

22 TABULAR DATASETS										
EVALUATOR	AUC_{QLT}	$AULC_G$	ACC_G	$AULC_P(\downarrow)$	$rAUC_{QLT}$	$rAULC_G$	$rACC_G$	$rAULC_P$	AVG. RANK	
EAP	0.821	0.779	0.839	0.717	1.91	4.27	4.28	2.11	3.14	
RARITY	0.724	0.782	0.839	0.753	3.59	4.42	4.91	4.92	4.46	
LAVA	0.723	0.744	0.794	0.747	3.62	7.48	7.17	4.08	5.59	
$P_{y x} + NP_x$	0.676	0.758	0.815	0.771	4.93	6.16	6.23	6.16	5.87	
KNNSHAP	0.541	0.770	0.825	0.805	7.61	5.24	5.29	9.15	6.82	
RANDOMEV	0.502	0.773	0.827	0.809	8.25	4.92	5.33	9.72	7.06	
AME	0.498	0.772	0.827	0.809	8.53	5.05	5.37	9.75	7.17	
LOO	0.504	0.750	0.798	0.792	7.90	6.87	7.10	7.77	7.41	
P_x	0.554	0.703	0.768	0.752	6.77	10.39	9.29	4.69	7.78	
$P_{y x}$	0.533	0.712	0.748	0.753	8.20	10.56	10.66	4.30	8.43	
DATAOOB	0.513	0.729	0.768	0.785	8.48	9.39	9.84	7.43	8.78	
INF	0.434	0.742	0.795	0.816	10.29	7.78	7.37	10.40	8.96	
DATABANZHAF	0.415	0.736	0.789	0.817	10.92	8.47	8.16	10.53	9.52	

5.2 Experimental Results

Q1. EAP vs baselines at assigning quality scores. Figure 1 shows the methods’ mean AUC_{QLT} on both image (left) and tabular data (right). On images, EAP outperforms all baselines on 13 out of 18 datasets, achieving an average AUC_{QLT} significantly higher than LAVA and RARITY by 6 and 12 percentage points, as shown in Table 1. Also, EAP consistently obtains the lowest (best) average ranking positions (1.99 for $rAUC_{QLT}$). On tabular data, EAP obtains an average $AUC_{QLT} = 0.821$, which is around 10 percentage points higher than the runner-ups. Also, EAP outperforms LAVA and RARITY on 18 and 17 datasets and obtains the best average ranking (1.91).

Interestingly, only EAP, LAVA, RARITY, and $P_{y|x} + NP_x$ achieve performance better than random, while other methods get average AUC_{QLT} around 0.5, which highlights their inability to distinguish good and poor auxiliary anomalies consistently. As a second remark, EAP performs lower than random for the dataset TILE. This happens because the defective images are extremely different than the normal images, thus resulting in real anomalies falling in zero-density regions, which our method would categorize as unrealistic.

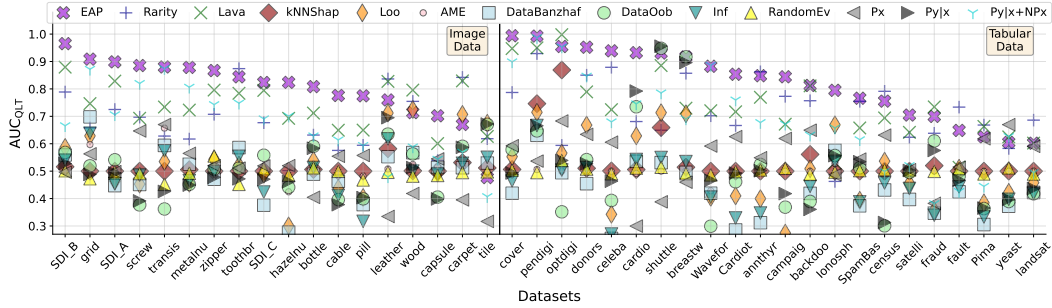


Figure 1: The plot illustrates the average AUC_{QLT} obtained by each method on a per-dataset basis (left for image data, right for tabular data). EAP achieves the highest (best) performance for most datasets, beating the runner-ups RARITY and LAVA on, respectively, 30 and 31 datasets out of 40.

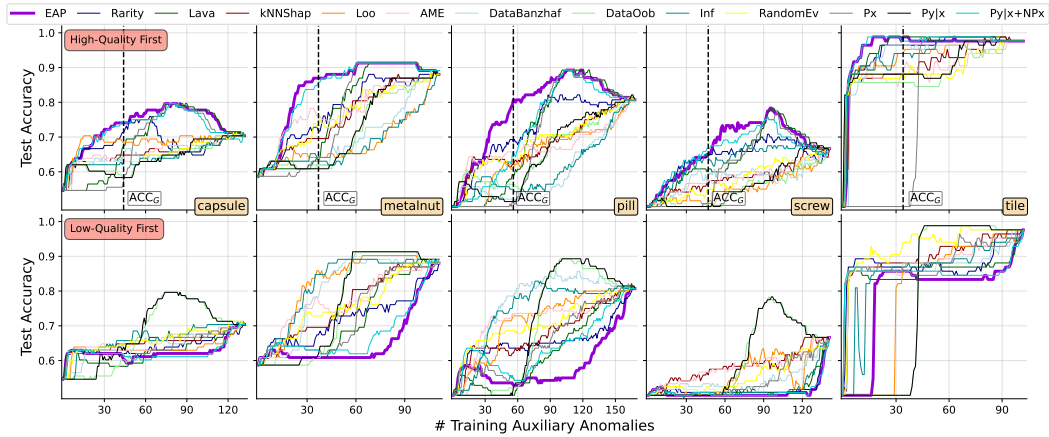


Figure 2: Learning curve (LC) obtained by following the method’s ordering (top) and inverse ordering (bottom) for five representative image datasets. Top: EAP’s LC_G grows sooner (i.e., better) than the other methods’, which confirms that including high-quality anomalies in the training set has a larger impact on the test performance. Bottom: EAP’s LC_P rises later (i.e., better) than most baselines’, showing that low-quality anomalies have a comparatively modest impact on the test performance.

Q2. Including high-quality anomalies in training. We measure how the performance of a model varies when introducing the top $\frac{1}{3}$ of auxiliary anomalies into the training following the methods’ rankings. Figure 2 (top) shows the learning curves (LC_G) for five representative image datasets. Overall, including high-ranked anomalies first has the claimed impact on the model’s performance: the learning curve grows sooner for EAP compared to all baselines. Consequently, EAP obtains an $AULC_G$ that is, on average, higher than all the baselines by between 2 (vs. RARITY and $P_{y|x} + NP_x$) and 5 (vs. LAVA) percentage points. After including one-third of the auxiliary anomalies for training, EAP shows an average improvement on the test performance (ACC_G) of 4 to 10 points over all baselines, standing out as the only method significantly better than RANDEEV. Moreover, Table 1 shows that EAP achieves the best average ranking for both $AULC_G$ (i.e., 3.94) and ACC_G (i.e., 3.12).

On tabular data, Table 1 shows that EAP achieves an average $AULC_G$ slightly lower than RARITY (0.779 vs 0.782) and a similar ACC_G (both 0.839). This occurs because, for most tabular datasets, RARITY assigns high-quality scores to the unrealistic anomalies which are obviously different than normal data. When including them for training, it yields an improvement of the RANDOM FOREST’s test accuracy surprisingly. From a ranking perspective, EAP obtains the lowest (best) average with $rAULC_G = 4.27$ (vs. RARITY’s 4.42), and $rACC_G = 4.28$ (vs. RARITY’s 4.91).

Q3. Including low-quality anomalies in training. Figure 2 (bottom) shows the LC_P obtained by following an inverse ordering of the methods, i.e., lower ranked anomalies are included first. Using this inverse ordering should result in much slower growth of the LC_P s: in some cases, the test accuracy using EAP remains stable (CAPSULE, METALNUT, SCREW), while in others it shows strong fluctuations going up and down quickly (PILL). Interestingly, every baseline’s performance

Table 2: Test AUCs (%) of prompt tuning with auxiliary anomalies selected by each baseline on MVTEC. EAP performs the best on 12 of 15 classes and achieves the highest average AUC.

Evaluator	bottle	cable	capsule	carpet	grid	hazel	leather	metal	pill	screw	tile	tooth	transis	wood	zipper	avg
KNNSHAP	82.4	56.7	51.4	82.1	58.8	72.7	92.1	51.7	49.1	60.2	69.2	77.0	77.1	72.7	44.7	66.5
AME	82.4	56.7	51.4	82.1	71.2	72.7	98.4	51.7	49.1	60.2	69.2	75.4	68.3	72.7	44.7	67.1
LOO	82.4	60.7	64.4	85.8	58.8	68.2	98.8	51.7	49.1	60.4	69.2	77.0	62.1	72.7	44.7	67.1
DATAOOB	82.4	60.7	63.7	85.8	71.2	72.7	98.8	51.7	49.1	60.4	69.2	75.4	62.1	72.7	44.7	68.0
$P_{y x}$	82.4	60.6	51.2	85.8	71.2	68.2	98.4	56.2	65.6	60.4	69.2	75.4	62.1	72.7	44.7	68.3
INF	95.3	56.7	45.7	96.1	83.6	68.2	98.8	51.7	65.7	60.4	69.2	75.4	62.1	93.0	75.9	73.2
DATABANZ	95.3	41.1	64.4	96.1	83.6	72.7	98.8	51.7	65.7	60.4	84.9	75.4	62.1	93.0	75.9	74.7
RANDOMEV	95.3	69.2	63.7	96.1	83.1	68.2	98.8	56.2	65.7	60.4	87.8	75.4	62.1	96.4	75.9	76.9
RARITY	94.3	69.2	64.4	96.1	83.6	83.8	98.8	45.1	63.5	60.4	91.8	75.4	77.1	96.4	75.9	78.4
P_x	94.3	70.2	64.6	96.1	83.6	76.7	86.9	90.8	63.5	60.4	84.9	75.4	77.1	93.0	75.9	79.6
LAVA	94.3	70.3	64.4	96.1	83.6	83.8	98.4	90.9	63.5	60.0	87.8	75.4	77.1	93.0	75.9	80.9
$P_{y x} + NP_x$	94.3	70.2	64.6	96.1	92.6	83.8	94.4	90.8	63.5	60.4	87.5	77.0	77.1	93.0	75.9	81.4
EAP	95.3	70.3	64.4	96.1	92.6	83.8	98.8	90.9	63.5	64.8	91.8	77.0	77.1	93.0	75.9	82.4

goes up for TILE: this is due to their poor ability to assign scores for this dataset, as described in Q1. Surprisingly, DATAOOB obtains the lowest (best) AUC_{LP} , while EAP has the second best AUC_{LP} with just two percentage points as gap. However, when ranking the experiments, EAP achieves the best average ranking (3.66 of $rAUC_{LP}$), thus being the preferred method for most of the experiments.

On tabular data, the results confirm the previous analysis: EAP has the lowest AUC_{LP} on 137 experiments out of 220, while RARITY and LAVA achieve so only on, respectively, 29 and 31 experiments. This motivates that EAP obtains an average AUC_{LP} that is better than all baselines by between 3 and 10 percentage points, as shown in Table 1.

Q4. Prompt tuning for zero-shot anomaly detection. CLIP-based anomaly detection methods save the effort of collecting training examples and enable a zero-shot anomaly detection [21]. However, their detection performance depends on the choice of prompts, which is usually tuned by using labeled real-world anomalies. We study the impact of selected auxiliary anomalies on prompt tuning for the MVTEC datasets. Specifically, we search a prompt for each object class achieving the best performance on the selected auxiliary anomalies from a pool of 27 candidate prompts (see details in Appendix A.3), and apply the best-performing prompt to CLIP at test time.

Table 2 reports the test AUCs of CLIP with the best-performing prompts selected by each data valuation method. We can see that EAP performs the best on 12 of 15 classes and achieves the highest AUC averaged over all classes. Thanks to accounting for both the class conditional probability and the data density, EAP clearly outperforms RARITY and P_x , which only consider the data density, $P_{y|x}$, which only considers the class conditional probability, and their naive linear combination $P_{y|x} + NP_x$. The results confirm that EAP selects high-quality auxiliary anomalies for the model selection purpose. We list the prompts selected by EAP in Appendix A.3.

Q5. EAP’ sensitivity to $\frac{\alpha_0}{\alpha_0 + \beta_0}$. EAP requires two hyperparameters: α_0, β_0 of the prior Beta distribution. To remove one degree of freedom, we set $\alpha_0 + \beta_0 = 1$ such that the dataset size n is much stronger (n times) than our initial belief. Then, we investigate how varying the parameter $\alpha_0 \in [0, 0.5)$ impacts EAP’s overall performance ($\beta_0 = 1 - \alpha_0$). We compare seven versions of our method by setting $\alpha_0 \in \{0.01, 0.05, 0.1, 0.2, 0.3, 0.4\}$, in addition to the original EAP that leverages the contamination level $\alpha_0 = m/n$. We call EAP_w the variant that uses $\alpha_0 = w$. Table 3 in the Supplement shows the rankings of these 7 variants for AUC_{QLT} and ACC_G and their average. Overall, both parameters have a low impact on our method: while a higher value for α_0 improves the AUC_{QLT} , in some experiments this improvement does not yield better performance at test time in terms of ACC_G . Moreover, setting α_0 too high or too low has inherent risks: $EAP_{0.4}$ and $EAP_{0.01}$ are the worst variants by far, with significant drops in performance compared to the other variants.

6 Conclusion and Limitations

This paper addressed the problem of evaluating the quality of an auxiliary set of synthetic anomalies. With this quality score, one can enrich an anomaly detection dataset to learn a more accurate anomaly detector. We proposed the expected anomaly posterior (EAP), the first quality score function for

auxiliary anomalies derived from an approximation for the posterior over the probability that a given input is an anomaly. We showed that our approach theoretically assigns higher scores to the realistic anomalies, compared to unrealistic and indistinguishable anomalies. Empirically, we investigated how EAP compares to adapted data quality estimators at (1) assigning quality scores, (2) using such scores to enrich the data for training, and (3) model selection. On 40 datasets, we show that EAP outperforms all 12 baselines in the majority of the cases.

Limitations. While our theoretical categorization refers to general anomalies, the concept of unrealistic/indistinguishable might be domain-driven and require adjustments in some applications (e.g., scratches on fabrics are unrealistic but would get high quality). Also, uncertainty-based methods require limited training samples to be effective and one may need to reduce the training normals.

Impact Statement. This paper presents work whose goal is to advance the field of Machine Learning. There are many potential societal consequences of our work, none of which we feel must be specifically highlighted here.

References

- [1] Y. Bengio, O. Delalleau, and N. Le Roux. The curse of dimensionality for local kernel machines. *Techn. Rep.*, 1258(12):1, 2005.
- [2] V. Bengs, E. Hüllermeier, and W. Waegeman. Pitfalls of epistemic uncertainty quantification through loss minimisation. *Advances in Neural Information Processing Systems*, 35:29205–29216, 2022.
- [3] V. Bengs, E. Hüllermeier, and W. Waegeman. On second-order scoring rules for epistemic uncertainty quantification. In *International Conference on Machine Learning*. PMLR, 2023.
- [4] L. Bergman and Y. Hoshen. Classification-based anomaly detection for general data. In *International Conference on Learning Representations*, 2020.
- [5] P. Bergmann, M. Fauser, D. Sattlegger, and C. Steger. Mvtec ad—a comprehensive real-world dataset for unsupervised anomaly detection. In *Proceedings of the IEEE/CVF conference on computer vision and pattern recognition*, pages 9592–9600, 2019.
- [6] V. Chandola, A. Banerjee, and V. Kumar. Anomaly Detection: A survey. *ACM computing surveys (CSUR)*, 41(3):1–58, 2009.
- [7] B. Charpentier, D. Zügner, and S. Günnemann. Posterior network: Uncertainty estimation without ood samples via density-based pseudo-counts. *Advances in Neural Information Processing Systems*, 33:1356–1367, 2020.
- [8] J. Chen, Y. Li, X. Wu, Y. Liang, and S. Jha. Atom: Robustifying out-of-distribution detection using outlier mining. In *Machine Learning and Knowledge Discovery in Databases. Research Track: European Conference, ECML PKDD 2021, Bilbao, Spain, September 13–17, 2021, Proceedings, Part III 21*, pages 430–445. Springer, 2021.
- [9] A. Deng, A. Goodge, Y. Lang, and B. Hooi. Cadet: calibrated anomaly detection for mitigating hardness bias. *IJCAI*, 2022.
- [10] P. Dhariwal and A. Nichol. Diffusion models beat gans on image synthesis. *Advances in neural information processing systems*, 34:8780–8794, 2021.
- [11] V. Feldman and C. Zhang. What neural networks memorize and why: Discovering the long tail via influence estimation. *Advances in Neural Information Processing Systems*, 33:2881–2891, 2020.
- [12] C. Fung, C. Qiu, A. Li, and M. Rudolph. Model selection of anomaly detectors in the absence of labeled validation data. *arXiv preprint arXiv:2310.10461*, 2023.
- [13] F. Gao, J. Li, R. Cheng, Y. Zhou, and Y. Ye. Connet: Deep semi-supervised anomaly detection based on sparse positive samples. *IEEE Access*, 9:67249–67258, 2021.

- [14] A. Ghorbani and J. Zou. Data shapley: Equitable valuation of data for machine learning. In *International conference on machine learning*, pages 2242–2251. PMLR, 2019.
- [15] I. Golan and R. El-Yaniv. Deep anomaly detection using geometric transformations. In *Advances in Neural Information Processing Systems*, pages 9758–9769, 2018.
- [16] J. Han, H. Choi, Y. Choi, J. Kim, J.-W. Ha, and J. Choi. Rarity score: A new metric to evaluate the uncommonness of synthesized images. *Proceedings of the International Conference on Learning Representations*, 2022.
- [17] S. Han, X. Hu, H. Huang, M. Jiang, and Y. Zhao. Adbench: Anomaly detection benchmark. In *Advances in Neural Information Processing Systems*, volume 35, pages 32142–32159, 2022.
- [18] D. Hendrycks, M. Mazeika, and T. Dietterich. Deep anomaly detection with outlier exposure. *Proceedings of the International Conference on Learning Representations*, 2019.
- [19] J. Ho, A. Jain, and P. Abbeel. Denoising diffusion probabilistic models. *Advances in neural information processing systems*, 33:6840–6851, 2020.
- [20] E. Hüllermeier and W. Waegeman. Aleatoric and epistemic uncertainty in machine learning: An introduction to concepts and methods. *Machine Learning*, 110:457–506, 2021.
- [21] J. Jeong, Y. Zou, T. Kim, D. Zhang, A. Ravichandran, and O. Dabeer. Winclip: Zero-/few-shot anomaly classification and segmentation. In *Proceedings of the IEEE/CVF Conference on Computer Vision and Pattern Recognition*, pages 19606–19616, 2023.
- [22] R. Jia, D. Dao, B. Wang, F. A. Hubis, N. M. Gurel, B. Li, C. Zhang, C. Spanos, and D. Song. Efficient task-specific data valuation for nearest neighbor algorithms. *Proc. VLDB Endow.*, 12(11):1610–1623, 2019.
- [23] K. F. Jiang, W. Liang, J. Zou, and Y. Kwon. Opendataval: a unified benchmark for data valuation. *Thirty-seventh Conference on Neural Information Processing Systems Datasets and Benchmarks Track*, 2023.
- [24] H. A. Just, F. Kang, J. T. Wang, Y. Zeng, M. Ko, M. Jin, and R. Jia. Lava: Data valuation without pre-specified learning algorithms. *Proceedings of the International Conference on Learning Representations*, 2023.
- [25] I. Kobyzev, S. J. Prince, and M. A. Brubaker. Normalizing flows: An introduction and review of current methods. *IEEE transactions on pattern analysis and machine intelligence*, 43(11):3964–3979, 2020.
- [26] H.-P. Kriegel, P. Kroger, E. Schubert, and A. Zimek. Interpreting and unifying outlier scores. In *International Conference on Data Mining*, pages 13–24, 2011.
- [27] Y. Kwon and J. Zou. Beta shapley: a unified and noise-reduced data valuation framework for machine learning. *International Conference on Artificial Intelligence and Statistics*, page 8780–8802, 2021.
- [28] Y. Kwon and J. Zou. Data-oob: Out-of-bag estimate as a simple and efficient data value. In *International Conference on Machine Learning*. PMLR, 2023.
- [29] A. Li, C. Qiu, M. Kloft, P. Smyth, S. Mandt, and M. Rudolph. Deep anomaly detection under labeling budget constraints. In *International Conference on Machine Learning*, pages 19882–19910. PMLR, 2023.
- [30] A. Li, C. Qiu, M. Kloft, P. Smyth, M. Rudolph, and S. Mandt. Zero-shot anomaly detection via batch normalization. In *Thirty-seventh Conference on Neural Information Processing Systems*, 2023.
- [31] J. Lin, A. Zhang, M. Lécuyer, J. Li, A. Panda, and S. Sen. Measuring the effect of training data on deep learning predictions via randomized experiments. In *International Conference on Machine Learning*, pages 13468–13504. PMLR, 2022.

- [32] F. T. Liu, K. M. Ting, and Z.-H. Zhou. Isolation forest. In *2008 eighth IEEE international conference on data mining*, pages 413–422. IEEE, 2008.
- [33] L. Martí, N. Sanchez-Pi, J. M. Molina, and A. C. B. Garcia. Anomaly Detection based on sensor data in petroleum industry applications. *Sensors*, 15(2):2774–2797, 2015.
- [34] Y. Ming, Y. Fan, and Y. Li. Poem: Out-of-distribution detection with posterior sampling. In *International Conference on Machine Learning*, pages 15650–15665. PMLR, 2022.
- [35] H. Murase and K. Fukumizu. Algan: Anomaly detection by generating pseudo anomalous data via latent variables. *IEEE Access*, 10:44259–44270, 2022.
- [36] G. Pang, C. Shen, L. Cao, and A. V. D. Hengel. Deep learning for anomaly detection: A review. *ACM computing surveys (CSUR)*, 54(2):1–38, 2021.
- [37] L. Perini, V. Vercruyssen, and J. Davis. Transferring the contamination factor between anomaly detection domains by shape similarity. In *Proceedings of the AAAI Conference on Artificial Intelligence*, volume 36, pages 4128–4136, 2022.
- [38] L. Perini, P.-C. Bürkner, and A. Klami. Estimating the contamination factor’s distribution in unsupervised anomaly detection. In *International Conference on Machine Learning*, pages 27668–27679. PMLR, 2023.
- [39] C. Qiu. *Self-Supervised Anomaly Detection with Neural Transformations*. PhD thesis, Rheinland-Pfälzische Technische Universität Kaiserslautern-Landau, 2023.
- [40] C. Qiu, T. Pfommer, M. Kloft, S. Mandt, and M. Rudolph. Neural transformation learning for deep anomaly detection beyond images. In *International Conference on Machine Learning*, pages 8703–8714. PMLR, 2021.
- [41] C. Qiu, M. Kloft, S. Mandt, and M. R. Rudolph. Raising the bar in graph-level anomaly detection. In *International Joint Conference on Artificial Intelligence*, 2022. URL <https://api.semanticscholar.org/CorpusID:249152138>.
- [42] C. Qiu, A. Li, M. Kloft, M. Rudolph, and S. Mandt. Latent outlier exposure for anomaly detection with contaminated data. In *International Conference on Machine Learning*, pages 18153–18167. PMLR, 2022.
- [43] L. Ruff, R. A. Vandermeulen, N. Görnitz, A. Binder, E. Müller, K.-R. Müller, and M. Kloft. Deep semi-supervised anomaly detection. *arXiv preprint arXiv:1906.02694*, 2019.
- [44] T. Silva Filho, H. Song, M. Perello-Nieto, R. Santos-Rodriguez, M. Kull, and P. Flach. Classifier calibration: a survey on how to assess and improve predicted class probabilities. *Machine Learning*, pages 1–50, 2023.
- [45] J. Soenen, E. Van Wolputte, L. Perini, V. Vercruyssen, W. Meert, J. Davis, and H. Blockeel. The effect of hyperparameter tuning on the comparative evaluation of unsupervised anomaly detection methods. In *Proceedings of the KDD’21 Workshop on Outlier Detection and Description*, pages 1–9. Outlier Detection and Description Organising Committee, 2021.
- [46] J. Tian, Y.-C. Liu, N. Glaser, Y.-C. Hsu, and Z. Kira. Posterior re-calibration for imbalanced datasets. *Advances in Neural Information Processing Systems*, 33:8101–8113, 2020.
- [47] V. Vercruyssen, W. Meert, G. Verbruggen, K. Maes, R. Baumer, and J. Davis. Semi-supervised anomaly detection with an application to water analytics. In *ICDM*, volume 2018, pages 527–536, 2018.
- [48] M. Verleysen and D. François. The curse of dimensionality in data mining and time series prediction. In *International work-conference on artificial neural networks*, pages 758–770. Springer, 2005.
- [49] B. C. Wallace and I. J. Dahabreh. Class probability estimates are unreliable for imbalanced data (and how to fix them). In *2012 IEEE 12th international conference on data mining*, pages 695–704. IEEE, 2012.

- [50] J. T. Wang and R. Jia. Data banzhaf: A robust data valuation framework for machine learning. In *International Conference on Artificial Intelligence and Statistics*, pages 6388–6421. PMLR, 2023.
- [51] R. Wang, S. Hoppe, E. Monari, and M. Huber. Defect transfer gan: Diverse defect synthesis for data augmentation. In *33rd British Machine Vision Conference 2022, BMVC 2022, London, UK, November 21-24, 2022*. BMVA Press, 2022.
- [52] R. Wang, S. Schmedding, and M. F. Huber. Improving the effectiveness of deep generative data. In *Proceedings of the IEEE/CVF Winter Conference on Applications of Computer Vision*, pages 4922–4932, 2024.
- [53] J. Yoon, S. Arik, and T. Pfister. Data valuation using reinforcement learning. In *International Conference on Machine Learning*, pages 10842–10851. PMLR, 2020.
- [54] X. Zhai, B. Mustafa, A. Kolesnikov, and L. Beyer. Sigmoid loss for language image pre-training. In *Proceedings of the IEEE/CVF International Conference on Computer Vision (ICCV)*, 2023.
- [55] Y. Zhou, X. Song, Y. Zhang, F. Liu, C. Zhu, and L. Liu. Feature encoding with autoencoders for weakly supervised anomaly detection. *IEEE Transactions on Neural Networks and Learning Systems*, 33(6):2454–2465, 2021.

A Supplement

A.1 Data quality estimators.

Any data quality estimator can be seen as a mapping that assigns a scalar score to any example (x, y) . Such a score quantifies the impact of (x, y) on the model’s performance when trained including the example in the training set. For this task, they introduce a utility function $U(\bar{D}) := \text{PERF}(f, \bar{D})$ that takes as input a subset \bar{D} of D and measures the performance of f when trained on it. Next, we briefly describe the existing data quality estimators employed in the experiments and refer to [23] for additional details.

- LEAVE ONE OUT (LOO) is defined as $\phi_{\text{LOO}}(x, y) = U(D) - U(D \setminus \{(x, y)\})$, where U is commonly chosen as the accuracy;
- DATASHAP generalizes LOO’s approach to the concept of marginal contributions, which measures the average change in utility when (x, y) is removed from any training set. Given a training set cardinality $j \leq N$, the marginal contribution is defined as

$$\mathcal{M}_j(x, y) := \binom{N-1}{j-1}^{-1} \sum_{\bar{D}_j \subseteq D, |\bar{D}_j|=j-1} U(\bar{D}_j \cup \{(x, y)\}) - U(\bar{D}_j)$$

where \bar{D}_j is a random subset of D of cardinality $j - 1$ that does not contain (x, y) . Then, DATASHAP [14] computes the score as $\phi_{\text{DATASHAP}}(x, y) = \frac{1}{N} \sum_{j=1}^N \mathcal{M}_j(x, y)$;

- BETASHAP [27] generalizes DATASHAP by considering a weighted average of marginal contributions $\phi_{\text{BETASHAP}}(x, y) = \frac{1}{N} \sum_{j=1}^N \omega_j \mathcal{M}_j(x, y)$, for some weights $\omega_1, \dots, \omega_N$.
- DATABANZHAF [50] exploits the same formulation as BETASHAP but sets the weights to $\omega_j = 2^{-N} \binom{N-1}{j-1}$.
- AME [31] shows that the average marginal contribution taken over random subsets of D can be efficiently estimated by predicting the model’s prediction. They employ a LASSO regression model that minimizes

$$\arg \min_{\gamma \in \mathbb{R}^N} \mathbb{E} [U(\bar{D}) - g(\mathbb{1}(\bar{D}))^T \gamma]^2 + \lambda \sum_{i=1}^N |\gamma_i|,$$

where $\mathbb{1}(\bar{D})$ is the multi-dimensional characteristic function, \bar{D} is a random subset draw the data distribution, λ is the regularization parameter, and $g: \{0, 1\} \rightarrow \mathbb{R}^N$ is a predefined transformation. The values γ_i represent the quality of (x_i, y_i) .

- KNNSHAP [22] differs from DATASHAP on the choice of the utility function:

$$U(\bar{D}) = \frac{1}{N_{\text{val}} k} \sum_{i=1}^{N_{\text{val}}} \sum_{(x_j, y_j) \in \mathcal{N}(x_i, \bar{D})} \mathbb{1}(y_i = y_j),$$

where k is the number of neighbors, N_{val} is the size of the validation set, and $\mathcal{N}(x_i, \bar{D})$ indicates the set of nearest neighbors for the validation example x_i over the subset \bar{D} . Roughly speaking, it measures the proportion of examples in \bar{D} that are neighbors of x_i and share the same label y_i .

- INFLUENCE FUNCTIONS (INF) [11] approximate the difference of utility functions in LOO by splitting D into two subsets of equal cardinalities and randomly drawing subsets from each of them:

$$\phi_{\text{INF}}(x, y) = \mathbb{E}_{\bar{D}_x} [U(\bar{D}_x)] - \mathbb{E}_{\bar{D}_{\neq x}} [U(\bar{D}_{\neq x})],$$

where all the subsets from \bar{D}_x contain (x, y) , while none of the subsets from $\bar{D}_{\neq x}$ contain (x, y) .

- LAVA [24] measures the quality of (x, y) by quantifying how fast the optimal transport cost between the training and validation sets changes when increasing more weight to (x, y) . That is,

$$\phi_{\text{LAVA}}(x, y) = h^* - \frac{1}{N-1} \sum_j h_j^*,$$

where h_i^* is part of the optimal solution of the transport problem.

- DATAOOB [28] relies on the concept of out-of-bag estimate to capture the data quality. Given B weak learners f_b , each trained on a bootstrap sample of D , the quality score is

$$\phi_{\text{DATAOOB}}(x, y) = \frac{\sum_{b=1}^B \mathbb{1}(w_b = 0) T(y, f_b(x))}{\sum_{b=1}^B \mathbb{1}(w_b = 0)},$$

where w_b is the number of times (x, y) is selected in the b -th bootstrap, and T is an evaluation metric (e.g., correctness $\mathbb{1}(y = f_b(x))$).

A.2 Rarity score

Formally, given a synthetic image with extracted feature x , the rarity score is a function $r_k: \mathbb{R}^d \rightarrow \mathbb{R}$ such that

$$r_k(x) = \begin{cases} 0 & \text{if } x \notin \bigcup_{x_i \in D} B_k(x_i) \\ \min_{x_i \in D: x \in B_k(x_i)} NN_k(x_i) & \text{otherwise} \end{cases} \quad (6)$$

where $NN_k(x_i)$ is the distance between x_i and its k -th nearest neighbor in D , and $B_k(x_i) = \{x | d(x_i, x) \leq NN_k(x_i)\}$ is the k -NN sphere with x_i as center and $NN_k(x_i)$ as radius. The rarity score strongly depends on the choice of the hyperparameter k : high values of k could map far unrealistic examples to a positive high score, namely they would be considered authentic, while low values of k could map real examples slightly different than the training data to a null score, namely they would be considered artifacts.

Because the rarity score strictly depends on the hyperparameter $k \in \{1, \dots, n-1\}$, we need to estimate a proper value \hat{k} . Let's assume the existence of an optimal k , and use the small set of m anomalies to estimate it. Ideally, k should be: (1) as low as possible to assign null scores to unrealistic anomalies, and (2) high enough to assign positive scores to the real training anomalies.

Following this insight, we assume a Bayesian perspective and set a normalized variable's K prior to be uniform

$$K := \frac{k-1}{n-1} \sim \text{BETA}(1, 1) = \text{UNIF}(0, 1).$$

Roughly speaking, we min-max normalize K to $[0, 1]$ to exploit that a Beta prior with a Bernoulli likelihood results in a Beta posterior distribution. Because we want the minimum k that assigns positive scores to the training anomalies $\{x_{\bar{m}}\}_{\bar{m} \leq m}$, we compute for each $x_{\bar{m}}$ the minimum $k_{\bar{m}}$ such that $r_{k_{\bar{m}}}(x_{\bar{m}}) > 0$. The set of normalized $\left\{\frac{k_{\bar{m}}-1}{n-1}\right\}_{\bar{m} \leq m}$ is the empirical evidence for the Bayesian update, which is

$$K \mid \left\{\frac{k_{\bar{m}}-1}{n-1}\right\} \sim \text{BETA}\left(1 + \sum_{\bar{m} \leq m} \frac{k_{\bar{m}}-1}{n-1}, 1 + m - \sum_{\bar{m} \leq m} \frac{k_{\bar{m}}-1}{n-1}\right).$$

Finally, we estimate \hat{k} as the 95th percentile of the posterior distribution of K

$$\hat{k} = \arg \min_{t \in [0, 1]} \mathbb{P}\left(K \mid \left\{\frac{k_{\bar{m}}-1}{n-1}\right\} \leq t\right) \geq 0.95 \quad (7)$$

which guarantees that at least 95% of real anomalies get a positive rarity score.

A.3 Prompt tuning for CLIP

```

%Candidate prompt templates for MvTec:
[ '{}', 'damaged {}'],
[ 'flawless {}', '{} with flaw'],
[ 'perfect {}', '{} with defect'],
[ 'unblemished {}', '{} with damage'],
[ '{} without flaw', '{} with flaw'],
[ '{} without defect', '{} with defect'],
[ 'a photo of a normal {}', 'a photo of an anomalous {}'],
[ 'a cropped photo of a normal {}', 'a cropped photo of an anomalous {}'],
[ 'a dark photo of a normal {}', 'a dark photo of an anomalous {}'],
[ 'a photo of a normal {} for inspection', 'a photo of an anomalous {} for inspection'],
[ 'a photo of a normal {} for viewing', 'a photo of an anomalous {} for viewing'],
[ 'a bright photo of a normal {}', 'a bright photo of an anomalous {}'],
[ 'a close-up photo of a normal {}', 'a close-up photo of an anomalous {}'],
[ 'a blurry photo of a normal {}', 'a blurry photo of an anomalous {}'],
[ 'a photo of a small normal {}', 'a photo of a small anomalous {}'],
[ 'a photo of a large normal {}', 'a photo of a large anomalous {}'],
[ 'a photo of a normal {} for visual inspection', 'a photo of an anomalous {} for visual inspection'],
[ 'a photo of a normal {} for anomaly detection', 'a photo of an anomalous {} for anomaly detection'],
[ 'a photo of a {}', 'a photo of something'],
[ 'a cropped photo of a {}', 'a cropped photo of something'],
[ 'a dark photo of a {}', 'a dark photo of something'],
[ 'a photo of a {} for inspection', 'a photo of something for inspection'],
[ 'a bright photo of a {}', 'a bright photo of something'],
[ 'a close-up photo of a {}', 'a close-up photo of something'],
[ 'a blurry photo of a {}', 'a blurry photo of something'],
[ 'a photo of a {} for visual inspection', 'a photo of something for visual inspection'],
[ 'a photo of a {} for anomaly detection', 'a photo of something for anomaly detection']

%EAP selected prompts for MvTec:
['bottle', 'damaged bottle'],
['cable without defect', 'cable with defect'],
['unblemished capsule', 'capsule with damage'],
['carpet', 'damaged carpet'],
['a bright photo of a normal grid', 'a bright photo of an anomalous grid'],
['hazelnut without defect', 'hazelnut with defect'],
['a photo of a normal leather for inspection', 'a photo of an anomalous leather for inspection'],
['metalnut', 'damaged metalnut'],
['pill', 'damaged pill'],
['a close-up photo of a screw', 'a close-up photo of something'],
['tile', 'damaged tile'],
['toothbrush without flaw', 'toothbrush with flaw'],
['a blurry photo of a normal transistor', 'a blurry photo of an anomalous transistor'],
['wood', 'damaged wood'],
['zipper without defect', 'zipper with defect']

```

Table 3: Comparison between EAP with default α_0 and its six variants EAP_w that set $\alpha_0 = w, \beta_0 = 1 - w$. Rankings show low sensitivity to such a choice, as long as $\alpha_0 < 0.4$.

EVALUATOR	rAUC _{QLT}	rACC _G	AVG. RANK
EAP	2.92	2.73	2.83
EAP _{0.2}	2.78	3.25	3.02
EAP _{0.3}	3.39	3.40	3.40
EAP _{0.1}	3.01	3.46	3.24
EAP _{0.05}	3.63	3.78	3.71
EAP _{0.01}	4.10	3.54	3.82
EAP _{0.4}	4.71	4.79	4.75

Table 4: Summary of the results obtained by the 13 methods over all 40 datasets. We report the mean \pm std, computed over all experiments. Overall, EAP achieves the best performance and ranking position for all evaluation metrics as well as the best average ranking (last column).

EVALUATOR	AUC _{QLT}	AULC _G	ACC _G	AULC _r (↓)	rAUC _{QLT}	rAULC _G	rACC _G	rAULC _r	AVG. RANK
EAP	0.81 \pm 0.13	0.76 \pm 0.15	0.84 \pm 0.14	0.70 \pm 0.14	1.95 \pm 1.65	4.12 \pm 2.88	3.76 \pm 2.75	2.82 \pm 2.17	3.16 \pm 1.67
RARITY	0.70 \pm 0.14	0.74 \pm 0.16	0.82 \pm 0.16	0.75 \pm 0.15	3.87 \pm 2.73	4.71 \pm 3.36	5.11 \pm 3.51	6.29 \pm 3.49	4.99 \pm 2.68
LAVA	0.73 \pm 0.13	0.71 \pm 0.16	0.78 \pm 0.17	0.73 \pm 0.14	3.21 \pm 2.03	7.79 \pm 3.63	7.29 \pm 3.62	4.36 \pm 2.54	5.66 \pm 2.19
$P_{y x} + NP_x$	0.67 \pm 0.18	0.73 \pm 0.16	0.81 \pm 0.16	0.75 \pm 0.14	4.82 \pm 3.22	5.87 \pm 3.40	5.90 \pm 3.37	6.55 \pm 3.22	5.79 \pm 2.53
LOO	0.52 \pm 0.17	0.72 \pm 0.16	0.79 \pm 0.16	0.75 \pm 0.14	7.59 \pm 3.48	6.42 \pm 3.57	6.86 \pm 3.31	7.04 \pm 3.42	6.98 \pm 2.90
KNNSHAP	0.53 \pm 0.08	0.74 \pm 0.16	0.81 \pm 0.15	0.78 \pm 0.15	8.05 \pm 2.02	5.74 \pm 2.84	5.59 \pm 2.60	9.28 \pm 2.36	7.16 \pm 1.40
RANDOMEV	0.50 \pm 0.06	0.74 \pm 0.16	0.81 \pm 0.15	0.79 \pm 0.15	8.55 \pm 2.43	5.50 \pm 2.63	5.60 \pm 2.45	9.80 \pm 2.21	7.36 \pm 1.66
AME	0.50 \pm 0.05	0.74 \pm 0.16	0.81 \pm 0.15	0.79 \pm 0.15	8.54 \pm 2.06	5.66 \pm 2.59	5.58 \pm 2.50	9.84 \pm 2.17	7.41 \pm 1.47
$P_{y x}$	0.52 \pm 0.14	0.69 \pm 0.16	0.73 \pm 0.16	0.70 \pm 0.13	8.69 \pm 3.10	9.66 \pm 3.07	10.64 \pm 2.46	3.73 \pm 2.67	8.18 \pm 2.13
DATAOOB	0.51 \pm 0.15	0.71 \pm 0.15	0.75 \pm 0.16	0.73 \pm 0.14	8.56 \pm 3.38	8.55 \pm 3.15	9.71 \pm 2.56	6.04 \pm 3.71	8.22 \pm 2.44
INF	0.46 \pm 0.14	0.71 \pm 0.16	0.79 \pm 0.17	0.78 \pm 0.14	9.65 \pm 2.61	7.43 \pm 3.17	7.08 \pm 2.95	9.56 \pm 2.79	8.43 \pm 2.26
P_x	0.53 \pm 0.11	0.63 \pm 0.15	0.69 \pm 0.16	0.74 \pm 0.14	7.59 \pm 3.59	11.28 \pm 2.68	10.38 \pm 3.32	6.06 \pm 3.27	8.83 \pm 2.51
DATABANZHAF	0.45 \pm 0.14	0.71 \pm 0.16	0.78 \pm 0.17	0.79 \pm 0.14	9.92 \pm 2.89	8.26 \pm 3.24	7.49 \pm 3.24	9.63 \pm 2.72	8.83 \pm 2.39